α decay of the neutron-deficient isotope ^{190}At

A. N. Andreyev,[1] D. Seweryniak,[2,*] B. Andel,[3] S. Antalic,[3] D. T. Doherty,[4] A. Korichi,[5] C. Barton,[1] L. Canete,[4]
M. P. Carpenter,[2] R. M. Clark,[6] P. A. Copp,[2] J. G. Cubiss,[1] J. Heery,[4] Y. Hrabar,[7] H. Huang,[8,9] T. Huang,[8] V. Karayonchev,[2]
F. G. Kondev,[2] T. Lauritsen,[2] Z. Liu,[8,9] G. Lotay,[4] C. Müller-Gatermann,[2] S. Nandi,[2] C. Page,[1] D. H. Potterveld,[2]
P. H. Regan,[4,10] W. Reviol,[2] D. Rudolph,[7] M. Siciliano,[2] R. S. Sidhu,[11] A. Sitarčík,[3] P. J. Woods,[11] Z. Yue,[1] and W. Zhang[8]

[1]*School of Physics, Engineering and Technology, University of York, York YO10 5DD, United Kingdom*
[2]*Argonne National Laboratory, Argonne, Illinois 60439, USA*
[3]*Department of Nuclear Physics and Biophysics, Comenius University in Bratislava, 84248 Bratislava, Slovakia*
[4]*School of Mathematics and Physics, University of Surrey, Guildford GU2 7XH, United Kingdom*
[5]*CNRS, IJCLab, Université Paris-Saclay, 91405 Orsay, France*
[6]*Lawrence Berkeley National Laboratory, Berkeley, California 94720, USA*
[7]*Department of Physics, Lund University, 22100 Lund, Sweden*
[8]*Institute of Modern Physics, Chinese Academy of Sciences, Lanzhou 730000, China*
[9]*School of Nuclear Science and Technology, University of Chinese Academy of Sciences, Beijing 100049, People's Republic of China*
[10]*Medical, Marine and Nuclear Department, National Physical Laboratory, Teddington TW11 0LW, United Kingdom*
[11]*School of Physics and Astronomy, University of Edinburgh, Edinburgh EH9 3JZ, United Kingdom*

The α decay of the neutron-deficient ^{190}At isotope was observed following the ^{103}Rh(^{90}Zr, 3n) ^{190}At reaction at Argonne National Laboratory. The reaction products were separated from the beam using the Argonne Gas-Filled Analyzer and implanted into a double-sided Si strip detector. The spatial and temporal correlations between implanted nuclei and subsequent α decays towards the known daughter isotope ^{186}Bi were used to identify and characterize ^{190}At nuclei. Two possible decay scenarios are proposed for the ^{190}At → ^{186}Bi decay.

I. INTRODUCTION

Neutron-deficient astatine ($Z = 85$) nuclei demonstrate a rich variety of shape coexistence and shape evolution phenomena. The ground states of the odd-A isotopes with $A \geqslant 197$ are usually associated with the occupation of the proton $\pi h_{9/2}$ orbital, leading to $J_{gs}^{\pi} = 9/2^-$ [1,2]. Moving away from the $N = 126$ shell closure towards the neutron-deficient side, the excitation energies of $1/2^+$ and $7/2^-$ states, where known, decrease as a function of the neutron number, resulting in low-lying $1/2^+$ isomers in ^{197,199,201,203}At. In the lighter isotopes ^{191,193,195}At, the $1/2^+$ state becomes the ground state, with the closely lying $7/2^-$ isomeric states at excitation energies as low as 50(30) keV in ^{191}At and 5(10) keV in ^{193}At [1]. These $1/2^+$ states have been interpreted as spherical-shell model intruder states, created by π(4p-1h) proton excitations across the $Z = 82$ shell gap, resulting in a proton hole in the $s_{1/2}$ orbital. Alternatively, in the deformed shell-model approach, such $1/2^+$ states are associated with the population of oblate-deformed Nilsson orbitals.

In the lightest known odd-odd ^{192,194,196}At isotopes, complex α-decay schemes were observed [3–5]. The odd proton is expected to occupy a $\pi h_{9/2}$, a $\pi f_{7/2}$, or a $\pi s_{1/2}$ state, coupled to the odd neutron in one of the low-lying $\nu p_{1/2}$, $\nu p_{3/2}$, $\nu f_{5/2}$,

or $\nu i_{13/2}$ orbitals, resulting in a multitude of closely spaced states. Similarly complex proton-neutron configurations also exist in the odd-odd Bi α-decay daughter isotopes. Details can be found in Table II in Ref. [4] for the ^{194}At / ^{190}Bi pair and in Refs. [6,7] for ^{184,186,188,190}Bi isotopes. In particular, two isomeric states were identified in ^{192}At [3]. The decay pattern of one of the isomers suggests that it is based on the oblate-deformed $\pi f_{7/2} \otimes \nu i_{13/2}$ configuration.

The changes in the mean-square charge radii of the At nuclei have been extracted from measured hyperfine-structure constants and isotope shifts [2]. The ground-state mean-square charge radii of the $^{194-198}$At isotopes strongly deviate from the trend of the spherical lead isotopes, which was interpreted as the result of an onset of oblate deformation when approaching the neutron midshell at $N = 104$, as also suggested by the macroscopic-microscopic calculations [8] shown in Fig. 1. Also, cases for shape coexistence have been identified in ^{197,199}At, for which a significant difference in the charge radii for near-spherical ($9/2^-$) ground states and isomeric ($1/2^+$) states has been observed. The latter confirms the deformed nature of the $1/2^+$ states. Interestingly, while the heavier isotopes ^{191,192}At are calculated to be oblate with $\beta_2 = -0.21$, ^{189,190}At are predicted to be prolate deformed with $\beta_2 = 0.30$ [8] (see Fig. 1).

As seen in the heavier At isotopes, several states decaying via α emission could exist in ^{190}At. The aim of this study was to search for the ^{190}At isotope and establish its decay properties.
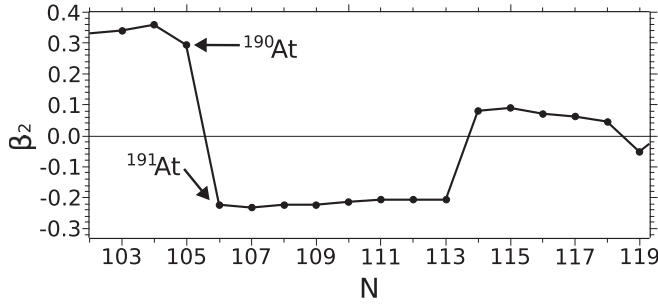
_____
*seweryniak@anl.gov

FIG. 1. Theoretical quadrupole ground-state deformation β_2 values for $^{188-204}$At isotopes based on the macroscopic-microscopic model [8].

II. EXPERIMENTAL DETAILS

^{190}At nuclei were synthesized using the ^{103}Rh(^{90}Zr, 3n) ^{190}At fusion-evaporation reaction. A ^{90}Zr beam with an energy of 410 MeV and an average beam intensity of 25 pnA was delivered on target for 77 h by the ATLAS accelerator at Argonne National Laboratory. The beam energy was chosen to obtain the maximum production of ^{190}At (3n) and ^{190}Po (p2n) evaporation channels. Four self-supporting 0.9- to 1.0-mg/cm^2-thick ^{103}Rh targets were mounted on a target wheel with a 17-mm radius. The wheel rotation frequency was about 1200 rpm. The beam was periodically swept away to avoid hitting the target wheel spokes. The recoiling reaction products were separated from the beam in the Argonne Gas-Filled Analyzer (AGFA) [9] and then passed through a parallel grid avalanche counter (PGAC) before they were implanted into a 300-μm-thick 64×64 mm^2 double-sided Si strip detector (DSSD). The AGFA was filled with He gas at a pressure of 0.47 Torr and magnetic fields were set to a value corresponding to a magnetic rigidity of $B\rho = 1.56$ Tm. A 2.6-mg/cm^2-thick Ni degrader was placed between the PGAC and the DSSD to slow down the reaction products. Slits were used at the exit from the AGFA to reduce the amount of scattered primary beam in the DSSD. The front and back sides of the DSSD were divided into 160 strips each, which were mutually orthogonal, resulting in 25 600 pixels. The implant energies and subsequent α-decay energies were measured in the same pixel. The decay times were determined by temporal and spatial correlations between implants and decays. An array of eight 4×7 cm^2 300-μm-thick single-sided Si strip detectors (SSSD), which formed a tunnel, was mounted upstream from the DSSD. They were used to detect α particles escaping from the DSSD. To veto energetic light particles such as protons and He ions, a 300-μm-thick 5×5 cm^2 Si detector was placed behind the DSSD. The energy resolutions (full width at half maximum) for the DSSD and the SSSD were 20 and 90 keV, respectively. The DSSD strips were calibrated using ^{240}Pu and ^{244}Cm α sources. The calibration was adjusted using energies of α particles emitted by α emitters produced in the experiment (see Fig. 2). This small correction accounted for the DSSD dead layer, which impacted the α-source measurement, and for the recoil energy of the α-decay daughter nucleus following the α-decay, which impacted the measured α-particle energies.
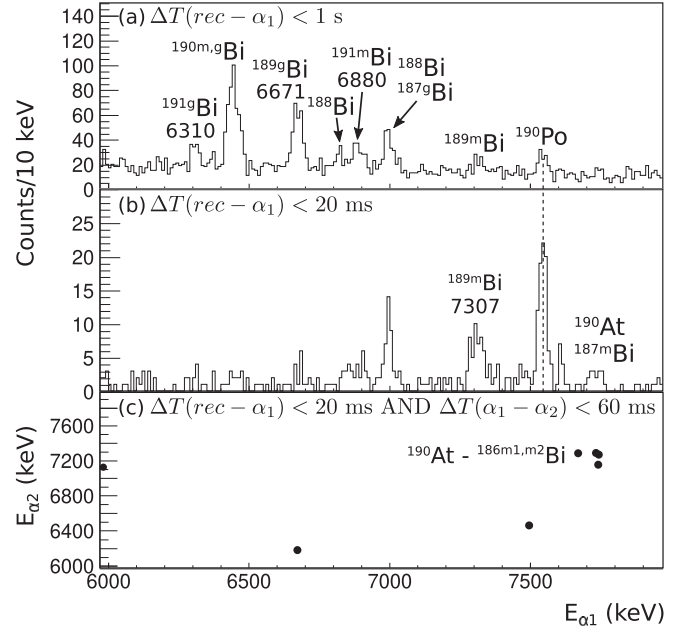

FIG. 2. Energy spectra of first generation α_1-decay events following recoil implantation within (a) 1 s and (b) 20 ms, respectively. The peaks are labeled with their energies (in keV) and the nuclide they originate from. (c) Correlation between the energies of first and second generation α decays, $\Delta t(\alpha_1$-$\alpha_2) \leqslant 60$ ms.

III. RESULTS

In the data analysis, the recoiling reaction products were selected by placing a gate on the energy deposited in the DSSD and the time of flight between coincident PGAC and DSSD signals. The events without coincidences with the PGAC were assumed to be decay events. Subsequently, decay chains were searched for following recoil implantation in the same DSSD pixel.

Figure 2(a) shows the energy spectrum of the first generation α_1 decays following recoils within 1 s. The $^{187-191}$Bi isotopes are strongly produced via the channels with the evaporation of two protons (e.g., ^{191}Bi) and/or an α particle and several neutrons. Note that the actual production of these isotopes is much higher than that seen in Fig. 2(a), as their α-decay lines are suppressed due to respective branching ratios and relatively long half-lives. The measured α-particle energies for all nuclei match well, within a few keV, with the literature values. Figure 2(b) focuses on the short-lived decay events within 20 ms after recoil implantation. This clearly demonstrates the production of ^{190}Po in the p2n channel and the presence of a small peak at around 7.72–7.75 MeV. The latter comprises the decay events from short-lived ^{187m}Bi ($T_{1/2} = 0.37$ ms, $E_\alpha = 7721$ keV [10]) and from ^{190}At, as shown below.

Based on the number of counts in the respective α lines (^{190}Bi and ^{190}Po) or the number of α-α correlations (^{190}At) and after implementation of the necessary corrections, the following production cross sections were deduced: 0.13 nb for ^{190}At, 2.9 nb for ^{190}Po, and 145 nb for ^{190}Bi. In the calculations, the nominal AGFA transmission of $\approx 50\%$ was

TABLE I. The list of observed recoil-α_1-α_2 correlations for ^{190}At, with measured decay energies and times.

Chain	$E\alpha_1$/keV	$E\alpha_2$/keV	Δt(ER-α_1)/ms	$\Delta t(\alpha_1$-$\alpha_2)$/ms
1	7746(10)	7149(10)	0.808	17.883
2	7743(10)	7252(10)	6.192	5.930
3	7673(40)[a]	7270(10)	3.089	25.848
4	7734(40)[a]	7271(40)[a]	2.291	2.252

[a]Energy of the α particle was shared between the DSSD and the tunnel detector.

decreased by a factor of 2, to account for the estimated fraction of the recoils stopped by the slits at the exit from the AGFA that were used to block the tail of the primary beam as described earlier. The uncertainty of the cross section cited above is about 50%.

Figure 2(c) shows α_1-α_2 correlations between energies of first and second generation decays following recoils with timing conditions of Δt(recoil-α_1) $\leqslant$ 20 ms and $\Delta t(\alpha_1$-$\alpha_2)$ $\leqslant$ 60 ms, respectively. A cluster of four events is clearly visible in Fig. 2(c). The decay energies and times associated with these events are given in Table I. The decay properties of the second generation decays in the cluster are consistent with the decays of two α-emitting states in ^{186}Bi [7]. As their relative energy is not known, we refer to them as ^{186m1,m2}Bi, similar to how they are referred to in Ref. [7]. Consequently, these four events were interpreted as ^{190}At - ^{186}Bi α-decay chains.

Below, we consider two different scenarios for the decay of ^{190}At shown in Fig. 3. In scenario 1, shown in Fig. 3(a), we assume the existence of only one α-decaying state in ^{190}At, because the energies of all four α_1 decays are quite similar. Based on the four observed events, a value of $T_{1/2}(^{190}$At) = $2.15^{+2.15}_{-0.72}$ ms was deduced in this case. However, for chain 1, the energy of the second α decay is 7149 keV, i.e., lower by about 120 keV compared to the remaining three events. This energy deviation is significant considering the energy

resolution of the DSSD. The energy of 7149 keV matches well to the literature value of 7152 keV for the strongest decay of ^{186m2}Bi, as can be seen in Fig. 3(a). On the other hand, the α_2 energies of the remaining decay chains 2–4 fit well to the literature value of 7263 keV for the main α decay of ^{186m1}Bi. Due to the small number of decay events and the similarity of the half-lives of ^{186m1,m2}Bi, the information on decay times for α_2 decays in the ^{190}At chains cannot be used to distinguish between the isomers. Therefore, based on the difference in the α_2 energies for chain 1 versus chains 2–4, we tentatively suggest that the single state of ^{190}At decays to two different states in ^{186}Bi, as shown in Fig. 3(a).

In scenario 2, shown in Fig. 3(b), we assume the existence of two α-decaying states in ^{190}At, each decaying to a specific daughter, ^{186m1,m2}Bi, in analogy to ^{192,194}At [3,4]. In this case, the respective half-lives, deduced based on 1 and 3 decay chains, are $T_{1/2}(^{190m2}$At) = $0.56^{+2.69}_{-0.26}$ ms and $T_{1/2}(^{190m1}$At) = $2.67^{+3.65}_{-0.98}$ ms, respectively.

IV. DISCUSSION

We now turn to the discussion of reduced α-decay widths δ_α^2, deduced using the Rasmussen formalism [11] for $\Delta L = 0$ decays and including screening corrections.

In scenario 2 [cf. Fig. 3(b)] both $\delta_\alpha^2(^{190m1,m2}$At) values are large, albeit with large experimental uncertainties, and comparable to respective values for the unhindered $1/2^+ \rightarrow 1/2^+$ and $7/2^- \rightarrow 7/2^-$ α decays in the neighboring ^{191,193}At nuclei. For the latter, the typical values are in the range of 60–150 keV (see Table 4 of Ref. [1]). Actually, all the above-mentioned values are also well comparable to those for the strongest decays of the ^{186m1,m2}Bi daughter isotope, as seen in Fig. 3, and also to the unhindered decays in odd-A ^{187,189}Bi [1,7]. This fact suggests that the properties such as spin, parity, and deformation of the parent ^{190m1,m2}At states are similar to those of the daughter ^{186m1,m2}Bi states, respectively. Unfortunately, due to presently unknown spin-parity assignments for ^{186m1,m2}Bi, no specific conclusion on these quantities can be drawn for ^{190m1,m2}At.

Because of the low statistics, we cannot exclude that the parent decays feed yet unknown low-lying excited states in ^{186m1,m2}Bi, instead of feeding directly their α-decaying states as shown in Fig. 3. Such unhindered fine-structure α decays are abundant in odd-odd At and Bi isotopes in this region [3,4].

In scenario 1 [cf. Fig. 3(a)], the decay branch to ^{186m1}Bi is unhindered, which suggests the similar structure of ^{190}At and this daughter state. In contrast to this, the decay branch to ^{186m2}Bi is weakly hindered by a factor of 3.7 relative to the other branch. The latter establishes some difference between ^{190}At and ^{186m2}Bi states, in agreement with the existence of two different α-decaying states in the daughter nucleus.

V. CONCLUSIONS

In summary, this study reports on the measurement of the decay properties of the exotic isotope ^{190}At. Four α-decay chains have been observed, suggesting two possible decay
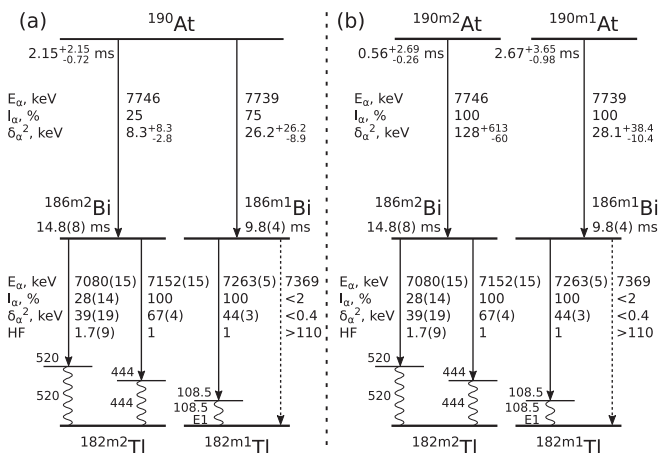
FIG. 3. Two proposed scenarios for the ^{190}At level scheme. See text for details. Decay schemes for the states in the daughter ^{186}Bi isotope were taken from Ref. [7].

scenarios. Because of the low number of events and yet unclear decay properties of the daughter ^{186}Bi isotope, no preference can be given to either of them. Future experiments with higher statistics will help to establish more detailed decay properties for ^{190}At and ^{186}Bi and will provide information on exotic nuclei above the $Z = 82$ closure.

Note added in proof. ^{190}At has been independently studied by Kokkonen *et al.* [12].

ACKNOWLEDGMENTS

[1] H. Kettunen, T. Enqvist, T. Grahn, P. Greenlees, P. Jones, R. Julin, S. Juutinen, A. Keenan, P. Kuusiniemi, M. Leino, A.-P. Leppänen, P. Nieminen, J. Pakarinen, P. Rahkila, and J. Uusitalo, Eur. Phys. J. A **17**, 537 (2003).

[2] J. G. Cubiss, A. E. Barzakh, M. D. Seliverstov, A. N. Andreyev, B. Andel, S. Antalic, P. Ascher, D. Atanasov, D. Beck, J. Bieron, K. Blaum, C. Borgmann, M. Breitenfeldt, L. Capponi, T. E. Cocolios, T. Day Goodacre, X. Derkx, H. De Witte, J. Elseviers, D. V. Fedorov *et al.*, Phys. Rev. C **97**, 054327 (2018).

[3] A. N. Andreyev, S. Antalic, D. Ackermann, S. Franchoo, F. P. Hessberger, S. Hofmann, M. Huyse, I. Kojouharov, B. Kindler, P. Kuusiniemi, S. R. Lesher, B. Lommel, R. Mann, G. Munzenberg, K. Nishio, R. D. Page, J. J. Ressler, B. Streicher, S. Sáro, B. Sulignano *et al.*, Phys. Rev. C **73**, 024317 (2006).

[4] A. N. Andreyev, S. Antalic, D. Ackermann, L. Bianco, S. Franchoo, S. Heinz, F. P. Heßberger, S. Hofmann, M. Huyse, I. Kojouharov, B. Kindler, B. Lommel, R. Mann, K. Nishio, R. D. Page, J. J. Ressler, P. Sapple, B. Streicher, S. Sáro, B. Sulignano *et al.*, Phys. Rev. C **79**, 064320 (2009).

[5] V. L. Truesdale, A. N. Andreyev, L. Ghys, M. Huyse, P. Van Duppen, S. Sels, B. Andel, S. Antalic, A. Barzakh, L. Capponi, T. E. Cocolios, X. Derkx, H. De Witte, J. Elseviers, D. V. Fedorov, V. N. Fedosseev, F. P. Heßberger, Z. Kalaninová, U. Köster, J. F. W. Lane *et al.*, Phys. Rev. C **94**, 034308 (2016).

[6] A. N. Andreyev, D. Ackermann, S. Antalic, H. J. Boardman, P. Cagarda, J. Gerl, F. P. Heßberger, S. Hofmann, M. Huyse, D. Karlgren, A. Keenan, H. Kettunen, A. Kleinböhl, B. Kindler, I. Kojouharov, A. Lavrentiev, C. D. O'Leary, M. Leino, B. Lommel, M. Matos *et al.*, Eur. Phys. J. A **18**, 39 (2003).

[7] A. N. Andreyev, D. Ackermann, F. P. Heßberger, S. Hofmann, M. Huyse, I. Kojouharov, B. Kindler, B. Lommel, G. Münzenberg, R. D. Page, K. Van de Vel, P. Van Duppen, and K. Heyde, Eur. Phys. J. A **18**, 55 (2003).

[8] P. Möller, A. Sierk, T. Ichikawa, and H. Sagawa, At. Data Nucl. Data Tables **109-110**, 1 (2016).

[9] B. B. Back, EPJ Web Conf. **163**, 00003 (2017).

[10] A. N. Andreyev, S. Antalic, D. Ackermann, S. Franchoo, F. P. Heßberger, S. Hofmann, M. Huyse, I. Kojouharov, B. Kindler, P. Kuusiniemi, S. R. Lesher, B. Lommel, R. Mann, G. Münzenberg, K. Nishio, R. D. Page, J. J. Ressler, B. Streicher, S. Sáro, B. Sulignano *et al.*, Phys. Rev. C **73**, 044324 (2006).

[11] J. O. Rasmussen, Phys. Rev. **113**, 1593 (1959).

[12] H. Kokkonen, K. Auranen, J. Uusitalo, S. Eeckhaudt, T. Grahn, P. T. Greenlees, P. Jones, R. Julin, S. Juutinen, M. Leino, A.-P. Leppänen, M. Nyman, J. Pakarinen, P. Rahkila, J. Sarén, C. Scholey, J. Sorri, and M. Venhart, Phys. Rev. C **107**, 064312 (2023).